

EFFECT OF COMBINED MAGNETIC NANO PARTICLE AND MANNICH BASE IN PHENOLIC WASTEWATER TREATMENT

V. Vanitha¹, N. Latha*

¹Researcher scholar, Dept. of Chemistry, Kanadswami Kandar's College, P. Velur, Namakkal Tamilnadu, India

* Asst. professor, Dept. of Chemistry, Kanadswami Kandar's College, P. Velur, Namakkal Tamilnadu, India

*Corresponding author: drshanmugaselvan@gmail.com

ABSTRACT

Present study concentrated on the preparation of combined Mannich base with magnetic nano particle by condensation method. Various techniques were employed to confirm the formation of mannich base. The base is combined with magnetic nano particle and used to treat the phenolic effluent like o- cresol, 2-chlorophenol, 2, 6-dichlorophenol. Mannich base alone give 80.75% of removal after 4 days, when it mixed with magnetic Nanoparticle the result is remarkable it gives 94.14% removal in 1hr.

Key words: Mannich, OTUB, FTIR, O- cresol

INTRODUCTION

It is well known that Mannich bases have powerful anti-inflammatory, anticancer, antifilarial, antibacterial, antifungal, anticonvulsant, anthelmintic, antitubercular, analgesic, anti-HIV, antimalarial, antipsychotic, and antiviral effects. These substances are employed as detergent additives, resins, polymers, and surface active agents in addition to their biological functions. Mannich base's potent antimicrobial properties are used to remove heavy metals from waste water. It is already common practise to treat leather, paper, and textiles, as well as the water used in the petroleum sector, with Mannich bases such 1-(morpholino (phenyl) methyl) pyrrolidine-2, 5-dione, morpholine, succinimide, and Benzaldehyde, 1, 3-bis-(morpholin-4-yl-phenyl-methyl)-thiourea. Additionally, used to remove heavy metals from effluents in the analytical reagents, cosmetics, and dye industries^{1,2}.

The removal of phenolic effluent, which cannot be treated by conventional coagulation and flocculation agents, is accomplished in industrial settings by the use of magnetic nanoparticles such as Fe₂O₃, MnO₂, and ferrotitanate².

There are three significant processes for producing iron oxide nanoparticles: physical, chemical, and biological. The fundamental benefit of magnetic nanoparticles is their ability to produce huge amounts of material while allowing for precise control over particle size (2–20 nm) and shape through the manipulation of pH, ionic strength, and solution concentration. Magnetic field-coated silica Nano adsorbents boost adsorption efficiency and provide stability³.

Heavy metal ions such as Cd(II), Co(II), Cu(II), Mn(II), Ni(II), and Pb(II) from water samples are detected using magnetite nanoparticles functionalized with silica and complexed with 8-hydroxy quinoline⁴. In this work, mannich base, which is already employed as a treatment agent, is used as a combination material in place of silica.

MATERIALS AND METHODS

Pure Tin Oxide Nanoparticle Preparation

To make a pure sample (1M), 11.28g of tin chloride is dissolved in 50 ml of double-distilled water and agitated for roughly an hour and a half. During this time, 15 ml of 3M aqueous ammonia solution is added dropwise, and after an hour, the mixture gels. The solution is then heated to cause the water molecules to evaporate, and it is then dried for roughly an hour at 80°C in a hot air oven. A pure sample is produced by calcining the material at 400°C. Samples are kept for doping and analysis.

Making of Material Doped with Mn

Tin oxide sample that has already been made is combined with 0.1M MnSO₄ and polyethylene glycol (PEG 600). The sample is dried and purified using the same process. Then the structure was analysed with XRD and FTIR.

RESULTS AND DISCUSSION

XRD

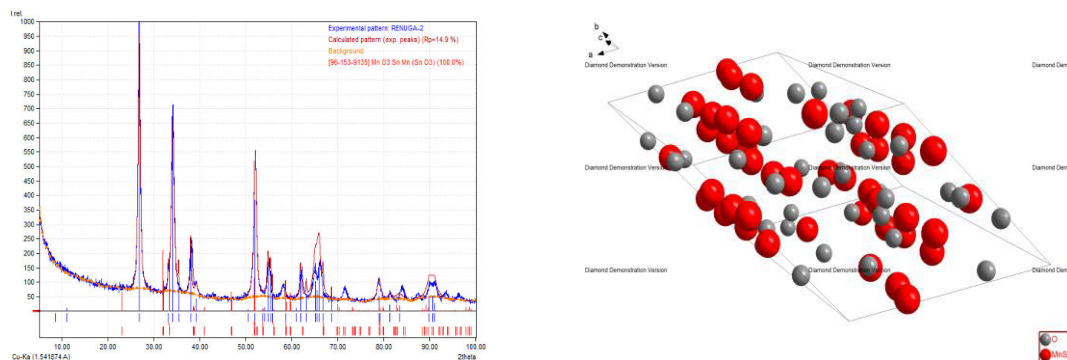


Fig. 1: XRD analysis

Trigonal (rhombohedral axis) structure with R-3C space group is visible for doped samples. With the aid of XRD, the following is how doping causes the hkl values to change: A sample that has been doped with 0.1M Mn exhibits high intensity peaks at d-value 2.8005 Å (211) and 2.8720 Å (10-1). The change in hkl value indicates that the sample contains doping (4). When doping occurs, impurities are added to the parent material, and as a result, the parent material's lattice structure is altered. When we introduce a known impurity into parent material, lattice disorder occurs because of the lattice disorder, which changes the morphology of the parent material⁵.

Synthesis procedure of 1-(phenyl(o-tolylamino) methyl) urea (OTUB)

Mannich condensation reaction between 1,2,4-triazole, succinimide, and formaldehyde in a 1:1:1 molar ratio produces 1-(Phenyl(O-Tolylamino) Methyl) Urea (OTUB). The equimolar ratio of O-toluidine (1.07mL, 0.01N), urea (0.67 gm, 0.01N), and benzaldehyde (1.06mL, 0.01N) was used. Urea and O-Toluidine were produced and blended in a concentrated aqueous solution while being constantly stirred. Drops of benzaldehyde were added while the reactant mixture was continuously stirred. The combination initially took on a bright, creamy white hue before gradually changing into an adult, crystalline mass as the process continued. The product underwent suction filtration separation and many acetone washes. By slowly evaporating chloroform, the product was dried and recrystallized.

1-(phenyl (O-tolylamino) methyl) urea (OTUB) is a white substance that melts between 173 and 175 degrees Celsius (Fig. 2)). It is totally soluble in chloroform, dimethyl formamide, DMSO, etc. but insoluble in water. The yield's percentage was 86.20%.

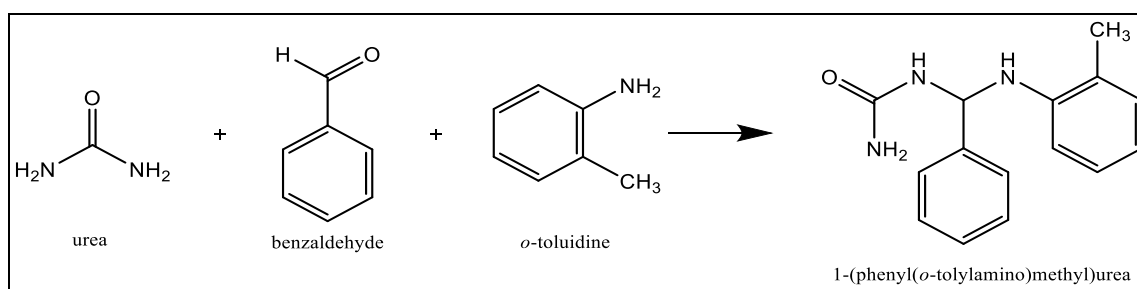


Fig-2: Formation of OTUB from reactant

Structural Characterization of OTUB

The compound's carbon, hydrogen, and nitrogen contents were examined. Below are the findings of the theoretical elemental analysis of OTUB.

Elemental Analysis

Table-1. Theoretical Elemental Analysis of OTUB

Elements	Calculated %
Carbon	70.56
Hydrogen	6.71
Nitrogen	16.46
Oxygen	6.27

The above Table-1 indicates the molecular formula of the compound as $C_{15}H_{17}N_3O$ and the molecular weight is 255.14.

Infrared spectral analysis (FTIR)

The OTUB infrared spectrum was captured on the KBr medium ($4000-400\text{ cm}^{-1}$) as depicted in Fig. 3. Table 2 lists the various stretching and bending frequency assignments for OTUB and compares them to those for urea and o-toluidine. The novel absorption bands found in the OTUB's IR spectra have multiple absorption bands, and their absorption frequencies are somewhat displaced from the reactants⁶.

This favourably indicates the substitution on O-Toluidine to diamide and formation of new compound. A sharp band observed at 3318 cm^{-1} is assigned to ν_{N-H} stretching vibration. The medium band at 3065 cm^{-1} is attributed to aromatic and 2923 cm^{-1} due to ν_{C-H} aliphatic stretching vibration. The band in the region of 1629 and 1585 cm^{-1} is due to $\nu_{C=C}$ in ring

stretching. The band at 1648 cm^{-1} due to $\nu_{\text{C=O}}$ stretching and the band at 1543 cm^{-1} $\nu_{\text{N-H}}$ out of plane. The medium band at 1201 cm^{-1} is due to the presence of $\nu_{\text{C-N-C}}$ stretching vibration. The absorption band appears at 1090 cm^{-1} in OTUB may be assigned to the stretching frequency of new $\nu_{\text{C-N-C}}$ bond formed due to the formation of Mannich base. The presence of absorption bands in the region $749\text{-}879\text{ cm}^{-1}$ is due to out of plane bending vibrations of δ C-H bonds of aromatic ring.

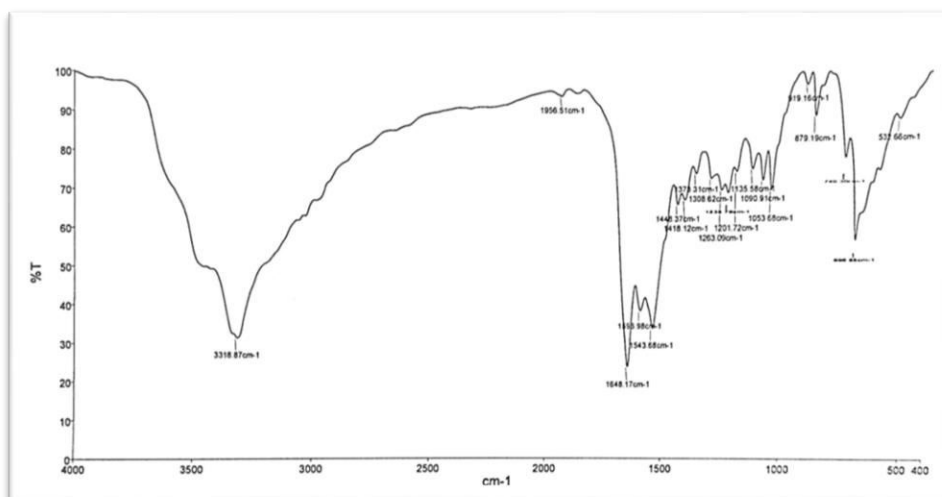


Fig. 3: FTIR Spectrum of OTUB

Table-2: Important IR absorption bands (cm^{-1}) of O-Toluidine, Urea and OTUB

O-Toluidine	Urea	OTUB	Tentative Assignment
3450	3447		
3367	3347	3318	
3219	3262	3318	ν_{OH}
-	-	-	ν_{NH}
3053	-	3065	ν_{CH} aromatic
3021	-	2923	ν_{CH} aliphatic
-	-	1956	$\nu_{\text{C=C}}$
-	-	1543	$\nu_{\text{C=N}}$
-	-	1448	$\nu_{\text{C-N}}$
-	-	1373	δ_{CH}
-	-	1308	$\nu_{\text{CN}}, \delta_{\text{CN}}$
-	-	1263,1201	ν_{Ring}
-	-	1135	$\nu_{\text{C-N-C}}$
-	-	1090	$\nu_{\text{C-N-C}}$ Newly formed
-	-	1053	$\nu_{\text{C-C}}, \delta_{\text{CH}_2}, \delta_{\text{ring}}$

-	-	919	δ_{CH} i.p.b benzene
-	-	879	δ_{CH_2} o.o.p ring
-	-	749, 532	698, δ_{CH} o.p.b benzene

The hazardous and non-biodegradable organic materials were treated using the produced nanoparticles in combination with mannich base. In order to determine the ideal pH, the sample was treated using the Jar test apparatus at various pH levels and for various lengths of time. The first time the magnetic nano particle was utilised to treat an organic pollutant was to remove the compounds O-Cresol, 2, 6-Chlorophenol, and 2-Dichlorophenol. The removal % was measured using the optical density method and the UV visible spectrum. Al_2O_3 nanoparticle serves as the standard in this investigation⁷.

Experimental procedure

The test water treatment is created in a 250 ml beaker; 2 mg of magnetic nanoparticles are introduced to 100 ml of mixed phenolic effluent at room temperature. For an even distribution of magnetic nanoparticles, the beaker is well-shacked. The nanoparticles are immobilised when an external magnetic field is applied. When stock solution is applied to 2 ml of the treated sample in a test tube, the sample's colour changes. The UV spectrum is used to quantify optical density. The process is repeated at various time intervals, and the table contains the observations. Mixed wastes are gathered and utilised to treat test water as well. Chemical o-cresol was treated with a combination of MNP and OTUB. Various concentrations were obtained and contrasted with a reference substrate⁸.

O-Cresol reduction experiments using mixed cultures

O-Cresol reduction experiment in wastewater was performed with five different initial concentrations (Ci) of cresol 50, 200, and 300 are common in industrial effluents and hence these concentrations were used. Some of the industrial effluents like petrochemical and coke oven effluents reports high concentration of o-cresols and for these reason studies were also performed for 500ppm of initial concentration. Compare the o-cresol degradation % for all using mixed MNP and standard. Following figures and charts shows the % degradation of o-cresol from 50ppm- 500ppm initial concentration (Table 3, 4& 5; Fig 4,5& 6). Also the pH changes indicate the removal of toxic compound from the rector. O- Cresol was acetic in nature, and the wastewater is also acetic, but after the treatment pH changes to neutral (7.0-7.89) from acetic. Cell viability test also carried out after the complete degradation. It also shows positive results⁹⁻¹¹.

Table 3: O- cresol degradation (mixed) for 50ppm

Name	1 Hr %	2Hr %	3Hr %	4Hr %
MNP & OTUB	3.768	23.82	81.56	94.14
$\text{Fe}_2\text{O}_3\text{Ti}$	7.68	77.15	89.21	91.18
Fe_2O_3 Mg	10.289	62.43	83.14	90.02
Al_2O_3	0.434	35.07	75.21	90.95
$\text{Ca}(\text{OH})_2$	45.945	61.15	72.95	92.17

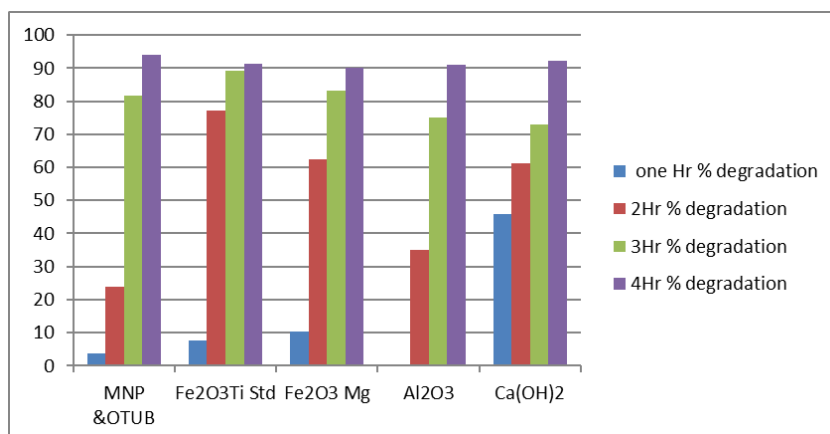


Fig. 4: 50ppm o-cresol removal by using mixed MNP

Table 4: O-cresol degradation (mixed) values for 200ppm

Reactor name	1 Hr %	2Hr %	3Hr %	4Hr %
MNP & OTUB	24.13	25.76	87.82	98.04
Fe₂O₃Ti Std	10.07	56.19	93.84	97.53
Fe₂O₃ Mg	86.44	96.41	88.62	99.05
Al₂O₃	86.49	92.28	90.14	95.43
Ca(OH)₂	17.24	94.23	92.75	97.6

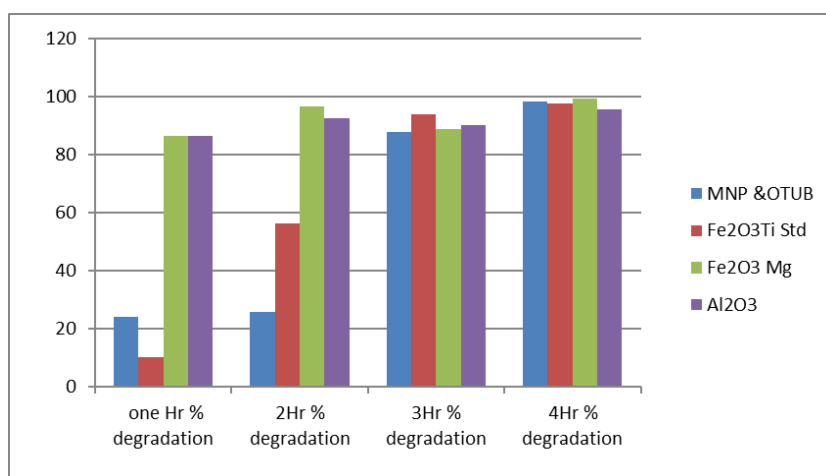


Fig. 5: 200ppm o-cresol removal using mixed MNP

Table. 5: O-Cresol degradation (mixed) values for 300ppm

Reactor name	1Hr %	2Hr %	3Hr %	4Hr %
MNP & OTUB	27.34	34.2	95.85	98.18
Fe₂O₃Ti Std	25.99	43.47	86.24	97.17
Fe₂O₃ Mg	8.21	6.763	22.41	58.62
Al₂O₃	9.08	8.691	88.56	97.63

Ca(OH)_2	3.38	14.02	78.59	94.9
-------------------	------	-------	-------	------

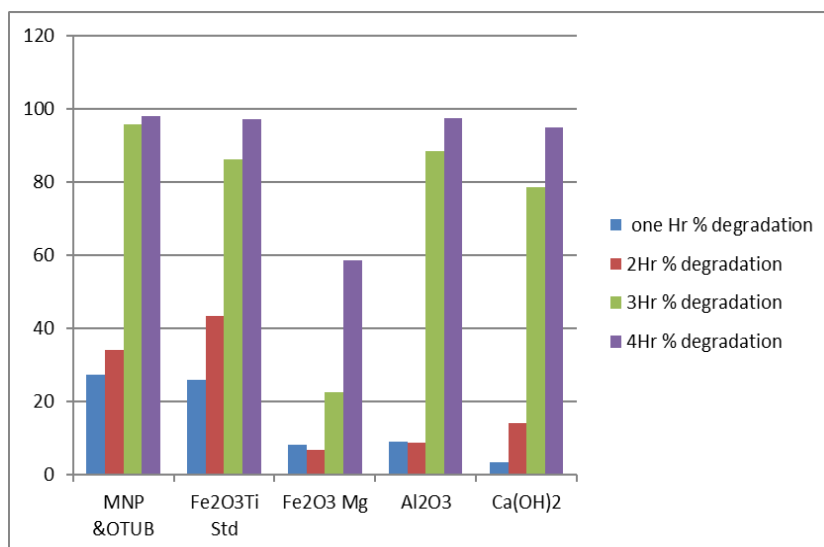


Fig. 6: 300ppm O-Cresol removal using mixed culture

CONCLUSION

The prepared OTUB and MNP were characterized by various instruments and confirmed their properties. From X-ray the prepared tin nano particle have R-3C and purity of sample was confirmed. The structure and composition of OTUB were confirmed with IR and elemental study.

In this study researcher tested potential treatment for wastewater containing o-cresol, and mixed effluent using mixed MNP & OTUB some other commonly available Flocculating agent. The results show the high potential applications in wastewater remediation. More than 90% of o-cresol removal was observed. Even for higher concentration (500ppm) of o-cresol.

REFERENCE

1. Suman T, Chakkaravarthi K, Elangomathavan R. Phyto-chemical profiling of *Cleistanthus collinus* leaf extracts using GC-MS analysis. *Research Journal of Pharmacy and Technology*. 2013; 6(11): 1173-1177p.
2. Bharati P and Pennarasi M. Production of Biodiesel from Municipal Sewage Sludge by Transesterification Process. *Biomass Valorization to Bioenergy*. 2019, 97–111.
3. Chakkaravarthi K, Gokulakrishnan K, Suman T, Tamilvendan D. Synthesize, Spectral, Antimicrobial and Antioxidant Studies of Mannich Bases of B-Naphthol and Gabapentin. *International Journal of ChemTech Research*. 2014; 6(1): 432-439p.
4. Chakkaravarthi K, Gokulakrishnan K, Suman T, Tamilvendan D. Synthesize, spectral, antimicrobial and antioxidant studies of diamide mannich base derivatives. *International journal of pharmacy and pharmaceutical sciences*. 2013; 6(1): 492-495p.
5. Shanmugaselvan R, Gokulakrishnan K. Preparation and Characterization of Mg Doped γ -Fe₂O₃ Prepared by Self-Propagation Method. *International Journal of Applied Chemistry* 2013; 9(3): 291-297p.
6. Selvan RS, Gokulakrishnan K. Effect of Doping in Magnetic Character in γ -Fe₂O₃ Nano Particle Elixir *Applied Chemistry*. 2017; 103:45526-45528p.
7. Bharathi P, Elavarasi N, Mohanasundaram S. Studies on rate of Biodegradation of Vegetable oil (Coconut oil) by using *Pseudomonas* sp. *International Journal of Environmental Biology*. 2012; 2(2): 12-19p.

8. Dave PN, Chopda LV. Application of Iron Oxide Nanomaterials for the Removal of Heavy Metals, *Journal of Nanotechnology*. 2014; 398569. DOI-10.1155/2014/398569.
9. Arockiaraj SP, Shanmugaselvan R, Pandiarajan A, et al. Effect of Doping in Copper Oxide Nanoparticles Studied by X-Ray Diffraction. *Bull. Env.Pharmacol. Life Sci*. 2022;(1): 397-402p.
10. Sulochana S, Soundaravalli K, Selvan RS. Effect of Aluminium, Magnesium Doping on Magnetic Nature of Zinc Oxide Nanoparticles Studied by X-Ray Diffraction Method. *Oriental Journal of Chem*. 2022; 38(3). DOI <http://dx.doi.org/10.13005/ojc/380310>
11. Rangarajan.N, Sampath.V, Dass Prakash MV, et al. UV Spectrophotometry and FTIR analysis of Phenolic Compounds with Antioxidant Potentials in *Glycyrrhiza glabra* and *Zingiber officinale*. *Int. J. Res. Pharm. Sci*. 2021;12(1):877-883.
- 12.